© 2014. Published by The Company of Biologists Ltd | Development (2014) 141, 269-280 doi:10.1242/dev.099622

RESEARCH ARTICLE

STEM CELLS AND REGENERATION

PRDM14 promotes active DNA demethylation through the Ten-eleven translocation (TET)-mediated base excision repair pathway in embryonic stem cells

Naoki Okashita[1,6,*], Yuichi Kumaki[2,*], Kuniaki Ebi[1,*], Miyuki Nishi[1], Yoshinori Okamoto[3], Megumi Nakayama[1], Shota Hashimoto[1], Tomohumi Nakamura[4], Kaoru Sugasawa[4], Nakao Kojima[3], Tatsuyuki Takada[5], Masaki Okano[2] and Yoshiyuki Seki[1,6,‡]

ABSTRACT

Ten-eleven translocation (TET) proteins oxidize 5-methylcytosine (5mC) to 5-hydroxymethylcytosine (5hmC), 5-formylcytosine (5fC) and 5-carboxylcytosine (5caC). 5fC and 5caC can be excised and repaired by the base excision repair (BER) pathway, implicating 5mC oxidation in active DNA demethylation. Genome-wide DNA methylation is erased in the transition from metastable states to the ground state of embryonic stem cells (ESCs) and in migrating primordial germ cells (PGCs), although some resistant regions become demethylated only in gonadal PGCs. Understanding the mechanisms underlying global hypomethylation in naive ESCs and developing PGCs will be useful for realizing cellular pluripotency and totipotency. In this study, we found that PRDM14, the PR domain-containing transcriptional regulator, accelerates the TET-BER cycle, resulting in the promotion of active DNA demethylation in ESCs. Induction of *Prdm14* expression transiently elevated 5hmC, followed by the reduction of 5mC at pluripotency-associated genes, germline-specific genes and imprinted loci, but not across the entire genome, which resembles the second wave of DNA demethylation observed in gonadal PGCs. PRDM14 physically interacts with TET1 and TET2 and enhances the recruitment of TET1 and TET2 at target loci. Knockdown of TET1 and TET2 impaired transcriptional regulation and DNA demethylation by PRDM14. The repression of the BER pathway by administration of pharmacological inhibitors of APE1 and PARP1 and the knockdown of thymine DNA glycosylase (TDG) also impaired DNA demethylation by PRDM14. Furthermore, DNA demethylation induced by PRDM14 takes place normally in the presence of aphidicolin, which is an inhibitor of G1/S progression. Together, our analysis provides mechanistic insight into DNA demethylation in naive pluripotent stem cells and developing PGCs.

KEY WORDS: DNA demethylation, Ten-eleven translocation (TET), Embryonic stem cells, Base excision repair (BER), Mouse

[1]Department of Bioscience, School of Science and Technology, Kwansei Gakuin University, 2-1 Gakuen, Sanda, Hyogo 669-1337, Japan. [2]Laboratory for Mammalian Epigenetic Studies, RIKEN Centre for Developmental Biology, 2-2-3 Minatojima-Minamimachi, Chuo-ku, Kobe 650-0047, Japan. [3]Faculty of Pharmacy, Meijo University, 150 Yagotoyama, Tempaku-ku, Nagoya 468-8503, Japan. [4]Biosignal Research Center, and Graduate School of Science, Kobe University 1-1 Rokkodai-cho, Nada-ku, Kobe, Hyogo 657-8501, Japan. [5]Laboratory of Cell Engineering, Department of Pharmaceutical Sciences Ritsumeikan, University Nojihigashi 1-1-1, Kusatsu, Shiga, Japan. [6]Research Center for Environmental Bioscience, Kwansei Gakuin University, 2-1 Gakuen, Sanda, Hyogo 669-1337, Japan.
*These authors contributed equally to this work

‡Author for correspondence (yseki@kwansei.ac.jp)

Received 30 May 2013; Accepted 14 October 2013

INTRODUCTION

DNA methylation at position 5 of cytosine (5mC) is a central epigenetic modification that plays crucial roles in embryonic development, genomic imprinting and X chromosome inactivation (Suzuki and Bird, 2008). In mammals, three DNA methyltransferases (DNMT1, DNMT3A and DNMT3B) coordinately establish and maintain the DNA methylation patterns of the genome (Li et al., 1992; Okano et al., 1999). DNMT3A and DNMT3B are developmentally regulated enzymes required for *de novo* DNA methylation during postembryonic development of mice. DNA methylation patterns established by DNMT3A and DNMT3B are accurately maintained by the DNMT1-UHRF1 complex, which recognizes hemimethylated CpG in newly synthesized DNA during cell division (Okano et al., 1999; Sharif et al., 2007).

DNA demethylation can occur through passive or active mechanisms. Passive DNA demethylation is triggered by inhibition of the maintenance activity of DNA methyltransferases during *de novo* DNA synthesis in DNA replication (Wu and Zhang, 2010). By contrast, hydroxylation of 5mC to 5-hydroxymethylcytosine (5hmC), catalyzed by the ten-eleven translocation (TET) proteins is the first step of active DNA demethylation through the base excision repair (BER) pathway in mammals (Hackett et al., 2012b). Deamination of 5hmC by activation-induced cytidine deaminase (AID; AICDA – Mouse Genome Informatics) produces 5-hydroxymethyluridine (5hmU), which can serve as a substrate for BER in cytosine regeneration (Guo et al., 2011). By contrast, a recent study has shown that C and 5mC, but not 5hmC, are substrates for AID, suggesting that the function of deaminases in active DNA demethylation is limited (Nabel et al., 2012). Alternatively, 5hmC is further oxidized to 5-formylcytosine (5fC) and 5-carboxylcytosine (5caC), which are both repaired by thymine DNA glycosylase (TDG) to produce unmodified cytosine (He et al., 2011; Ito et al., 2011). Although both oxidation from 5mC to 5hmC and from 5hmC to 5fC/5caC are catalyzed by the same TET proteins, the genomic content of 5hmC is much higher than that of 5fC/5caC in embryonic stem cells (ESCs), which suggests that the conversion of 5hmC to 5fC/5caC is tightly controlled through the regulation of TET protein activity. However, the molecular mechanisms underlying the regulation of TET protein activity in active DNA demethylation remain largely unknown.

In a previous study, we found that PRDM14 is a crucial regulator for specification of germ cell fate and proper genome-wide epigenetic reprogramming (Yamaji et al., 2008). In mice, *Prdm14* is expressed not only in primordial germ cells (PGCs), but also in the inner cell mass (ICM) and ESCs (Yamaji et al., 2008). *Prdm14*-deficient mice are infertile, but viable, providing evidence that *Prdm14* expression in the ICM is not required for pluripotency in

Development (2014) doi:10.1242/dev.099622

the ICM and during embryonic development. However, it has been shown that endogenous PRDM14 represses spontaneous differentiation of ESCs into extra-embryonic endoderm cells (Ma et al., 2011). Recent evidence suggests that the disruption of *Prdm14* leads to the differentiation of ESCs in the presence of leukemia inhibitory factor (LIF)-containing serum, but not in the presence of mitogen-activated protein kinase (MAPK) inhibitors, as these prime the differentiation of ESCs in response to FGF4 autocrine signals, whereas the glycogen synthase kinase 3 pathways destabilize the core transcription factor network through transcription factor 3 (TCF3) (in LIF-containing 2i medium) (Grabole et al., 2013; Yamaji et al., 2013). Furthermore, PRDM14 represses the DNA methylation machinery to maintain global hypomethylation in naive pluripotent stem cells.

PRDM14 is required not only for maintenance of ESC pluripotency, but also for specification and early differentiation of PGCs in mice (Yamaji et al., 2008). PGCs are specified from the most proximal epiblast cells, which is accompanied by the induction of two PR domain-containing transcriptional regulators, PRDM1 (also known as BLIMP1) and PRDM14, expressed at approximately embryonic day (E) 6.25 and E6.5, respectively (Ohinata et al., 2005; Yamaji et al., 2008). Our previous whole-mount immunofluorescence studies indicated that migrating PGCs erase global DNA methylation and histone H3 lysine 9 dimethylation (H3K9me2), after which H3K27me3 is induced at a genome-wide level during hindgut migration (Seki et al., 2005; Seki et al., 2007). Recent whole-genome bisulphite sequencing has shown that global loss of DNA methylation occurs in migrating PGCs, whereas some resistant regions become demethylated only in gonadal PGCs (Seisenberger et al., 2012). Active repression of *Dnmt3a*, *Dnmt3b* and *Uhrf1*, coupled with rapid proliferation of PGCs, might trigger replication-dependent passive demethylation in developing PGCs (Kagiwada et al., 2013; Ohno et al., 2013).

Recently, TET proteins have been implicated in DNA demethylation in PGCs. *Tet1*-deficient female mice show an abnormality in meiotic progression; this abnormality is caused by the decreased expression of a subset of meiotic genes associated with hypermethylation of their promoter region (Yamaguchi et al., 2012). Furthermore, aberrant hypermethylation at imprinted loci is observed in the progeny of *Tet1*/*Tet2* double knockout (DKO) mice, suggesting that *Tet1*/*Tet2* is required for proper erasure of genomic imprints in PGCs (Dawlaty et al., 2013). Interestingly, although the expression levels of *Tet1* and *Tet2* in PGCs are lower than those in ESCs (Kagiwada et al., 2013), erasure of genomic imprints is observed only in developing PGCs, suggesting that these cells might have some factors that are involved in the enhancement of TET-mediated DNA demethylation. In this study, we found that high expression of PRDM14, as observed in developing PGCs, promotes active DNA demethylation through the TET-BER pathway in pluripotency-associated genes, germline-specific genes and imprinted loci in ESCs.

RESULTS

PRDM14 induced DNA demethylation in pluripotency-associated genes, germline-specific genes and imprinted loci

To monitor the dynamics of 5mC and 5hmC regulated by PRDM14, we established ESCs in which the expression of *Prdm14* could be controlled by doxycycline (Dox). The levels of both *Prdm14* transcript and PRDM14 protein increased following treatment with Dox (Fig. 1A). The expression levels of *Prdm14* induced by Dox were much higher than those in naive ESCs but similar to those in developing PGCs (supplementary material Fig. S1A). Several recent studies have shown that endogenous PRDM14 represses the transcription of the DNA methylation machinery, *Dnmt3a*, *Dnmt3b* and *Dnmt3l*, which is involved in global hypomethylation in ESCs in the presence of LIF-containing 2i medium (Ficz et al., 2013; Grabole et al., 2013; Leitch et al., 2013; Yamaji et al., 2013). We observed rapid downregulation of *Dnmt3b* and *Dnmt3l* expression, but not *Dnmt3a* expression, soon after the induction of *Prdm14* expression (Fig. 1B; supplementary material Fig. S1B). Next, we monitored 5mC and 5hmC near the transcription start site (TSS) of the germline-specific genes *Piwil2*, *Mael* and *Sycp1*, because aberrant hypermethylation at those genes are observed in *Tet1* knockout (KO) PGCs (Yamaguchi et al., 2012). Glucosylation of genomic DNA followed by methylation-sensitive qPCR (GlucMS-qPCR) analysis, which can distinguish between 5mC and 5hmC, indicated that the 5mC levels near the TSS of *Mael*, *Sycp1* and *Piwil2* rapidly decreased following *Prdm14* induction (Fig. 1C). Furthermore, we observed transient enrichment of 5hmC levels near the TSS of *Piwil2*, *Mael* and *Sycp1* after *Prdm14* induction. We analyzed the methylation levels around the TSS of other germline-specific genes, major satellite DNA and IAP, which revealed that DNA methylation of germline-specific genes and major satellite DNA but not IAP were demethylated by PRDM14 induction (Fig. 1D). Consistent with the removal of 5mC near the TSS of germline-specific genes, we observed elevation of their mRNA levels after *Prdm14* induction (Fig. 1E; supplementary material Fig S1C). However, the expression levels of those genes in *Prdm14*-overexpressing ESCs and Dnmt triple KO (*Dnmt1*, *Dnmt3a*, *Dnmt3b*) ESCs were significantly lower than those in PGCs, suggesting that other factors in addition to PRDM14-dependent DNA demethylation are necessary to fully activate germline-specific genes in developing PGCs. We next measured the genome-wide methylation levels by *Hpa*II digestion and liquid chromatography-tandem mass spectrometry (LC-MS/MS) analysis. Genome-wide methylation of the *Hpa*II site was modestly reduced and the relative amounts of 5mC in total C of the genome slightly reduced after *Prdm14* induction (Fig. 1F,G). These findings provide evidence that induction of PRDM14 expression at a high level similar to developing PGCs erases DNA methylation at germline-specific genes but not across the entire genome in ESCs, resembling the second wave of demethylation in gonadal PGCs (Seisenberger et al., 2012).

Next, to monitor global changes in 5mC levels induced by PRDM14 overexpression in ESCs, we performed methylated DNA immunoprecipitation combined with high-throughput sequencing (MeDIP-seq). We selected three categories (pluripotency-associated genes, germline-specific genes and imprinted loci) and compared the 5mC levels of these genes in *Prdm14*-uninduced (–Dox) and *Prdm14*-induced (+Dox) ESCs. The 5mC near the TSS of *Tcl1*, *Tcfap2c* (*Tfap2c* – Mouse Genome Informatics) (pluripotency-associated genes), *Spo11* and *Sycp3* (germline-specific genes) was widely removed by PRDM14 overexpression (Fig. 2A). Leitch et al. had previously reported that genomic imprints are maintained in naive pluripotent stem cells (Leitch et al., 2013). By contrast, we observed extensive reduction of 5mC at imprinted loci after *Prdm14* induction. Recent global analyses of 5mC in developing PGCs have discovered regions resistant to demethylation in PGCs (Guibert et al., 2012; Hackett et al., 2012a; Seisenberger et al., 2012). Interestingly, the 5mC at or near the TSS of *Vmn2r29* (demethylation-resistant region in PGCs) also exhibited resistance to PRDM14-mediated DNA demethylation. To validate the results of MeDIP-Seq analysis, we performed GlucMS-qPCR on pluripotency-associated genes, germline-specific genes and

Development (2014) doi:10.1242/dev.099622

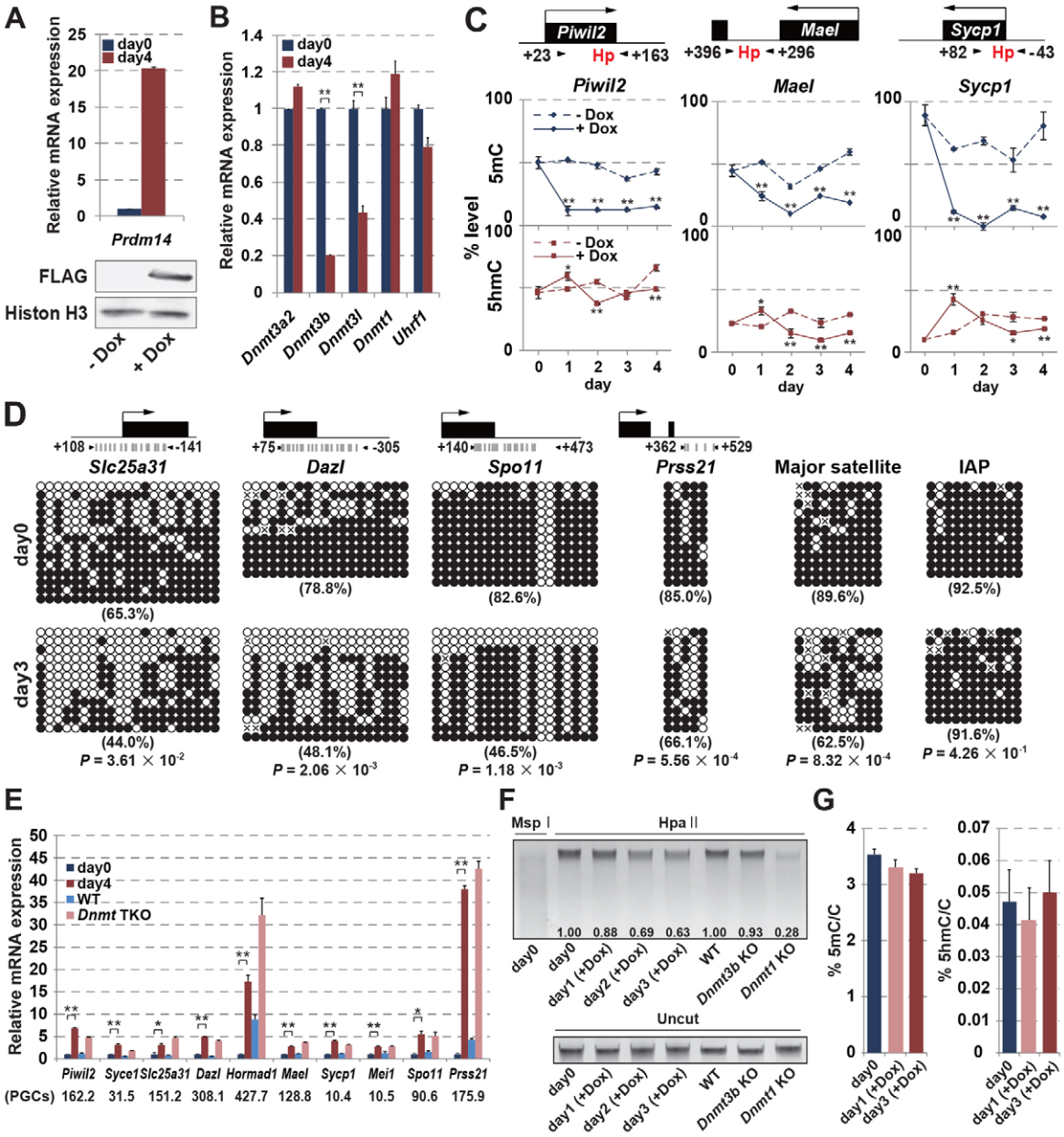

Fig. 1. PRDM14 induces DNA demethylation at germline-specific genes. (A) qRT-PCR analysis and western blotting analysis of Prdm14 in *Prdm14*-inducible ESCs with (day 4) or without (day 0) Dox. (B) qRT-PCR analysis of *Dnmt3a2*, *Dnmt3b*, *Dnmt1* and *Uhrf1* in *Prdm14*-inducible ESCs with (day 4) or without (day 0) Dox. (C) GlucMS-qPCR analysis at or near the TSS of *Piwil2*, *Mael*, and *Sycp1* in *Prdm14*-inducible ESCs with or without Dox. (D) Bisulphite sequence analysis (BS) around the promoter region of germline-specific genes, major satellite DNA and IAP. White circles indicate unmethylated cytosine, black circles indicate methylated cytosine and crosses indicate mutation of cytosine. (E) qRT-PCR analysis of germline-specific genes in *Prdm14*-inducible ESCs with (day 4) or without (day 0) Dox, wild-type and Dnmt TKO ESCs. The relative expression levels of germline-specific genes in PGCs (E12.5 female) are indicated below the graph. (F) *Hpa*II digestion of the genome derived from ESCs with or without Dox. (G) Mass spectrometric measurement of global 5mC and 5hmC level in ESCs with or without Dox. *P* values for qRT-PCR and GlucMS-qPCR were obtained using Student's *t*-test. **P*<0.05, ***P*<0.01. *P* values for BS were obtained using Mann–Whitney *U*-test. Error bars indicate s.e.m. values of technical duplicates of qPCR results.

imprinted loci in which the reductions of 5mC were detected after *Prdm14* induction by MeDIP-Seq. We observed consistent reduction of 5mC and elevation of 5hmC on those regions 1 day after *Prdm14* induction (Fig. 2B). To determine whether PRDM14 overexpression accelerates the conversion of metastable pluripotency to ground-state pluripotency in ESCs, we analyzed the expression of ground-state ESC-enriched genes (Marks et al., 2012). We found no elevation of ground state ESC-enriched genes in *Prdm14*-induced ESCs (supplementary material Fig. S1D), suggesting that the reduction in 5mC levels for the pluripotency-associated genes, germline-specific genes and imprinted loci after *Prdm14* induction is not caused by the conversion of metastable pluripotency to ground-state pluripotency in ESCs.

PRDM14 enhances the recruitment of TET proteins at target loci

The rapid kinetics of DNA demethylation by PRDM14 suggested that PRDM14 induces active DNA demethylation but not

Development (2014) doi:10.1242/dev.099622

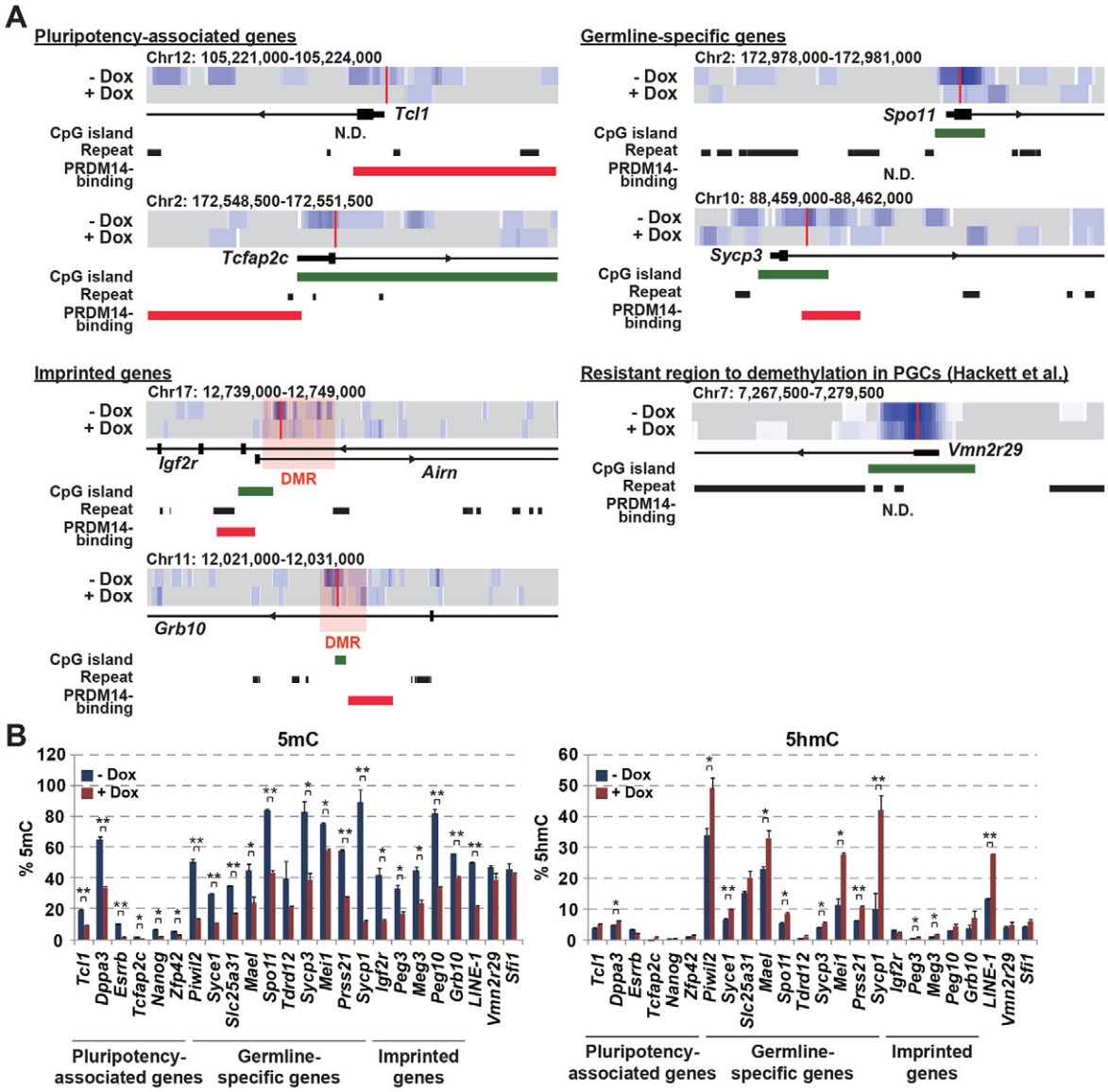

Fig. 2. PRDM14 induces DNA demethylation at pluripotency-associated genes, germline-specific genes and imprinted loci. (A) The heatmap represents the read densities of MeDIP-Seq surrounding the genomic regions of pluripotency-associated genes (*Tcl1*, *Tcfap2c*), germline-specific genes (*Spo11*, *Sycp3*), imprinted loci (*Igf2r*, *Grb10*) and demethylation-resistant region in PGCs. The red bar indicates PRDM14-binding regions in ESCs, as reported previously (Ma et al., 2011). The red line indicates the primer position for GlucMS-qPCR analysis. (B) Validation of the levels of 5mC and 5hmC by GlucMS-qPCR analysis of the genomic region of pluripotency-associated genes (*Tcl1*, *Dppa3*, *Esrrb*, *Tcfap2c*, *Nanog* and *Zfp42*), germline-specific genes (*Mael*, *Spo11*, *Tdrd12*, *Sycp3*, *Mei1* and *Prss21*), imprinted loci (*Igf2r*, *Peg3*, *Meg3*, *Peg10* and *Grb10*), LINE-1, and demethylation-resistant regions in PGCs (*Vmn2r29*, *Sfi1*) in *Prdm14*-inducible ESCs with Dox or without Dox. Error bars indicate s.e.m. values of technical duplicates of qPCR results. *P* values for GlucMS-qPCR were obtained using Student's *t*-test. **P*<0.05, ***P*<0.01. N.D., not detected.

replication-dependent passive DNA demethylation. 5mC oxidation by TET proteins is the first step of BER-mediated active DNA demethylation (Guo et al., 2011). We examined whether PRDM14 can interact with TET proteins by co-immunoprecipitation analysis, and found that both endogenous TET1 and TET2 were co-immunoprecipitated with overexpressed PRDM14 (Fig. 3A). We further mapped the interaction domain of PRDM14 with TET1 and TET2 by introducing different fragments of the PRDM14 protein in ESCs (Fig. 3B). The N-terminal domain of PRDM14 is required for physical interaction with TET1 and TET2 (Fig. 3C,D). Furthermore, the interaction of PRDM14 with TET1 and TET2 was impaired by the deletion of the C-terminal zinc finger domain, which can recognize a specific sequence of DNA (Ma et al., 2011). These findings suggest that PRDM14 interacts with TET1 through its N-terminal domain and that DNA binding of PRDM14 enhances this interaction. ChIP-Seq data of PRDM14 in ESCs have shown that endogenous PRDM14 weakly binds near the TSS of *Piwil2* and *Slc25a31* rather than with *Dnmt3b* distal regions (Fig. 4A) (Ma et al., 2011). Next, to investigate the recruitment of PRDM14, TET1 and TET2 at *Slc25a31* and *Piwil2*, in which 5mC was demethylated by PRDM14 overexpression, we performed chromatin immunoprecipitation analysis (ChIP) with anti-FLAG (PRDM14), anti-TET1 and anti-TET2 antibodies in the presence or absence of Dox (Fig. 4B). We detected the enrichment of PRDM14 binding at or near the TSS of *Slc25a31* and *Piwil2* loci with Dox treatment. TET1 and TET2 were already localized near TSS in the absence of

Development (2014) doi:10.1242/dev.099622

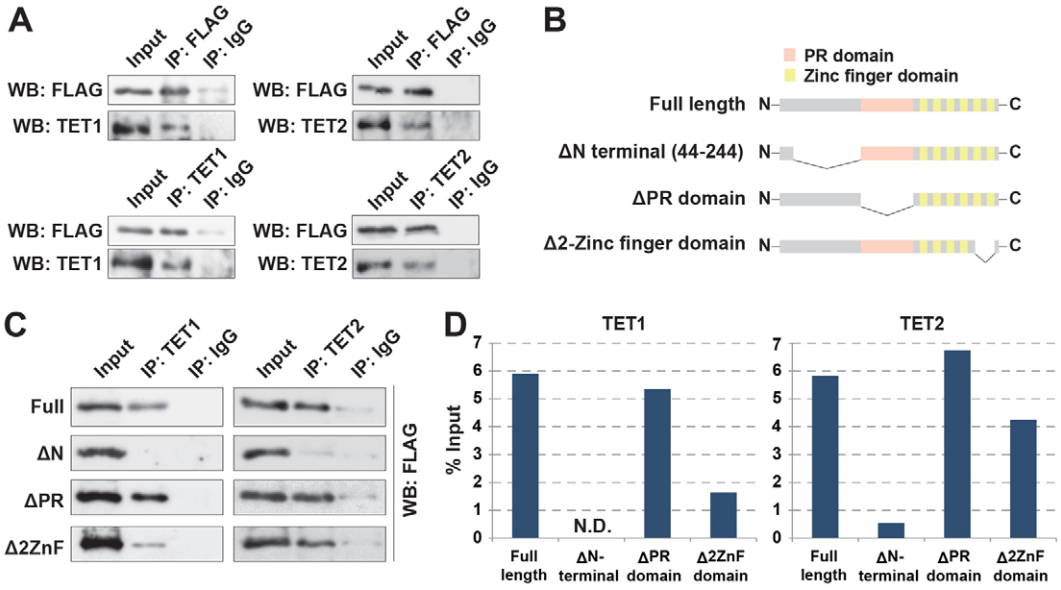

Fig. 3. PRDM14 interacts with TET1 and TET2 through its N-terminal domain. (A) Detection of interaction between overexpressed PRDM14 and endogenous TET1 and TET2 by co-immunoprecipitation analysis. (B,C) The interaction domain of PRDM14 with TET1 and TET2 was identified by co-immunoprecipitation analysis with the transient transfection of several deletion constructs of PRDM14 in ESCs. (D) Signal intensities of co-immunoprecipitated PRDM14 with TET1 and TET2 were calculated using ImageJ. N.D., not detected.

Dox. Interestingly, the recruitment of TET1 and TET2 was enhanced by the overexpression of PRDM14 at or near the TSS of *Slc25a31* and *Piwil2*. These cumulative data suggest that PRDM14 promotes the conversion of 5mC to 5hmC through the enhancement of TET1/2 recruitment at the target loci, which might trigger the erasure of DNA methylation. Next, we investigated the interaction of endogenous PRDM14 with TET1 and TET2 in ESCs cultured in LIF-containing 2i medium. We found that endogenous PRDM14

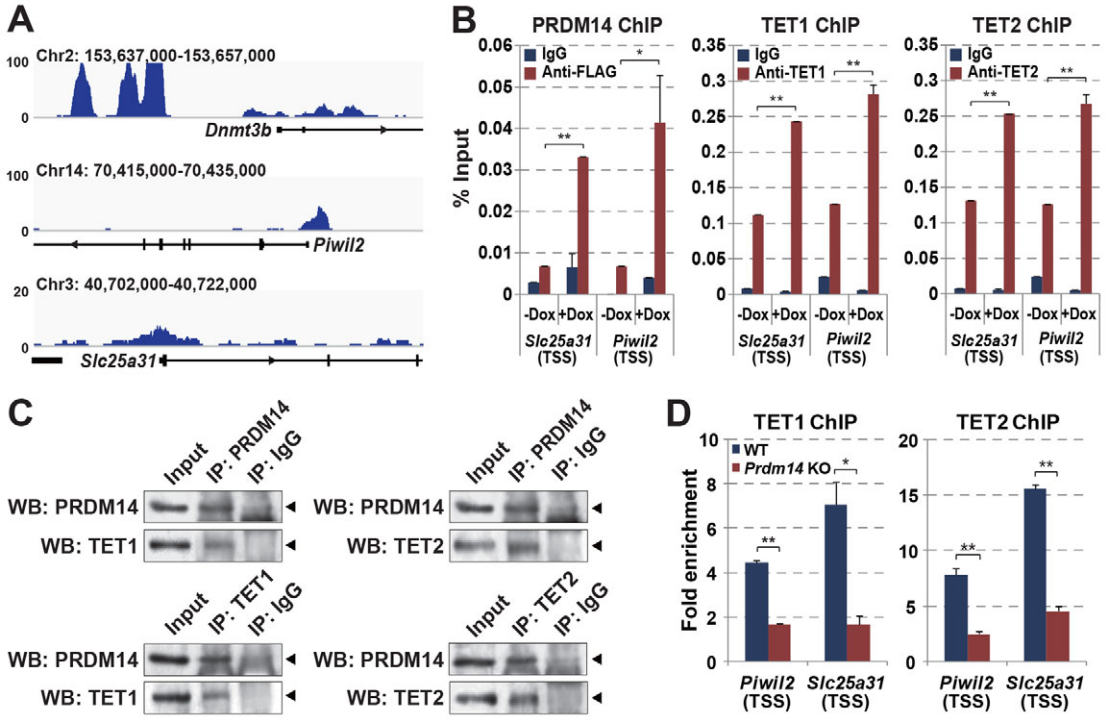

Fig. 4. Endogenous PRDM14 interacts with TET1 and TET2 and enhances the recruitment of TET1 and TET2 at target loci. (A) Analysis of endogenous PRDM14 binding on *Dnmt3b*, *Piwil2* and *Slc25a31* using ChIP-Seq data from Ma et al. (Ma et al., 2011). (B) ChIP analysis of PRDM14 (anti-FLAG), TET1 and TET2 at or near the TSS of *Slc25a31* and *Piwil2* in *Prdm14*-inducible ESCs with or without Dox. (C) Detection of interaction between endogenous PRDM14 and TET1 and TET2 in ESCs with LIF-containing 2i medium by co-immunoprecipitation analysis. (D) ChIP analysis of TET1 and TET2 at or near the TSS of *Slc25a31* and *Piwil2* in wild-type and *Prdm14* KO ESCs. Error bars indicate s.e.m. values of technical duplicates of qPCR results. *P* values for ChIP-qPCR were obtained using Student's *t*-test. **P*<0.05, ***P*<0.01.

Development (2014) doi:10.1242/dev.099622

interacts with TET1 and TET2 in ground-state ESCs (Fig. 4C), which suggests that PRDM14 facilitates the recruitment of TET1 and TET2 at germline-specific genes in ground-state ESCs. Therefore, we compared the enrichment of TET1 and TET2 at or near the TSS of *Slc25a31* and *Piwil2* in wild-type ESCs and *Prdm14* KO ESCs cultured in LIF-containing 2i medium by ChIP. The loss of *Prdm14* abrogated the enrichment of both TET1 and TET2 in ground-state ESCs (Fig. 4D).

DNA demethylation by PRDM14 depends on TET proteins

The results described above suggest that the promotion of TET1 and TET2 enrichment by PRDM14 overexpression at target loci accelerates BER-dependent active demethylation. To investigate the role of TET1 and TET2 in PRDM14-dependent DNA demethylation, we created TET1/TET2 double knockdown (*Tet1*/*Tet2* DKD) ESCs carrying Dox-inducible *Prdm14* expression units (Fig. 5A). To investigate the TET1 and TET2 dependency in

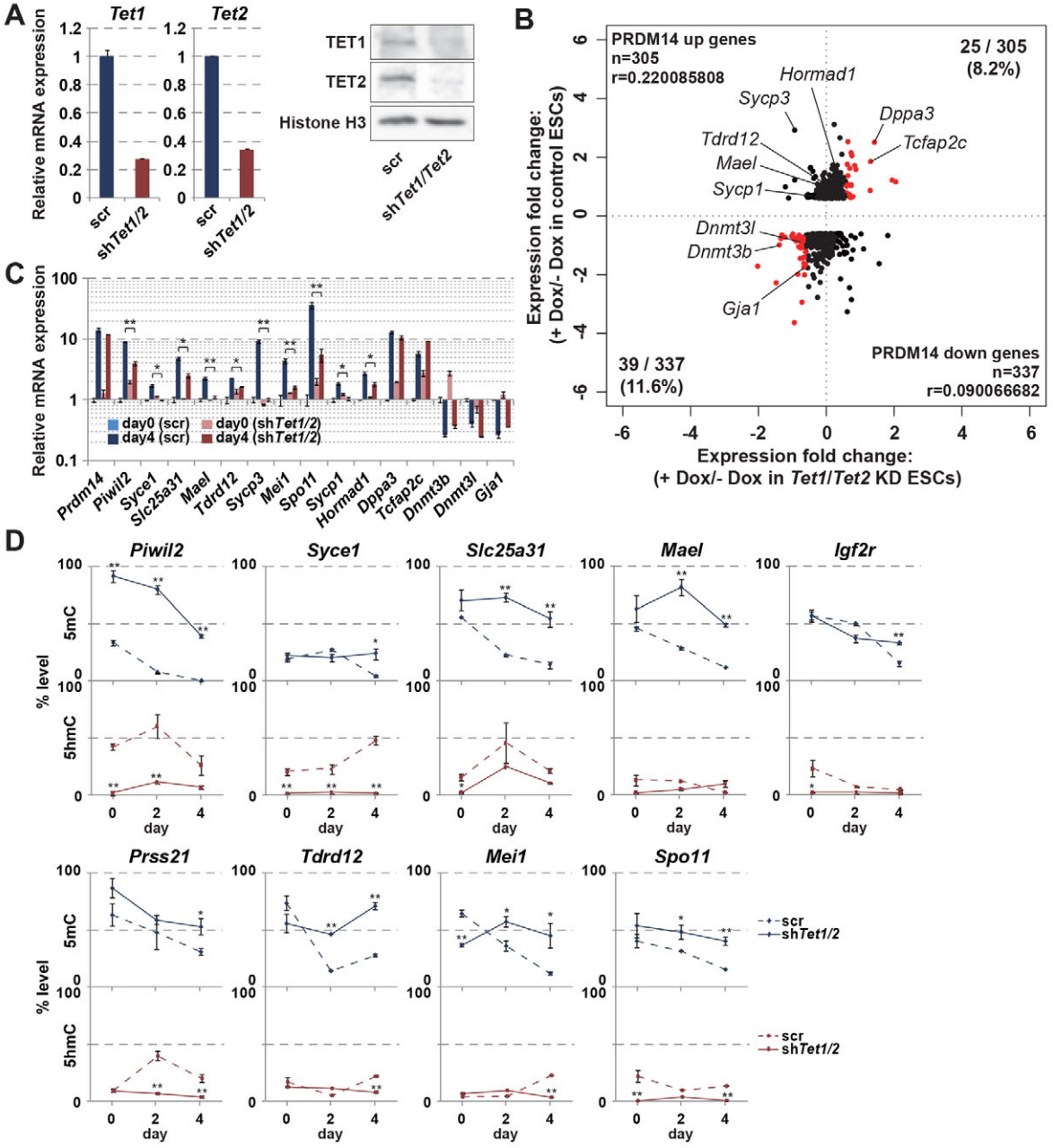

Fig. 5. PRDM14-dependent DNA demethylation depends on TET1 and TET2 functions. (A) Knockdown efficiencies of *Tet1* and *Tet2* were validated by qRT-PCR and western blotting. (B) Scatterplot of microarray data represents genes upregulated or downregulated by PRDM14 in control ESCs. The *y*-axis indicates fold changes between + Dox control ESCs and –Dox control ESCs by applying ≥1.5-fold difference as a cut-off value. The *x*-axis indicates a fold change between + Dox *Tet1*/*Tet2* KD ESCs and –Dox *Tet1*/*Tet2* KD ESCs. Red dots indicate genes upregulated or downregulated by PRDM14 both in the control and *Tet1*/*Tet2* KD ESCs. (C) qRT-PCR analysis of *Prdm14*, *Piwil2*, *Syce1*, *Slc25a31*, *Mael*, *Tdrd12*, *Sycp3*, *Mei1*, *Spo11*, *Sycp1*, *Hormad1*, *Dppa3*, *Tcfap2c*, *Dnmt3b*, *Dnmt3l* and *Gja1* in ESCs with scrambled shRNA and *Tet1*/*Tet2* shRNA after *Prdm14* induction. (D) GlucMS-qPCR analysis of 5mC and 5hmC levels at or near the TSS of *Piwil2*, *Syce1*, *Slc25a31*, *Mael*, *Igf2r*, *Prss21*, *Tdrd12*, *Mei1* and *Spo11* in ESCs with scrambled shRNA and *Tet1*/*Tet2* shRNA after *Prdm14* induction. Error bars indicate the s.e.m. values of technical duplicates of qPCR results. *P* values for qRT-PCR and GlucMS-qPCR were obtained using Student's *t*-test. **P*<0.05, ***P*<0.01.

Development (2014) doi:10.1242/dev.099622

the transcriptional regulation of PRDM14, we analyzed the global gene expression profiles of *Prdm14*-inducible ESCs with scrambled short hairpin (sh)RNA and *Tet1*/*Tet2* shRNA by microarray analysis. The majority of genes upregulated and downregulated by PRDM14, when applying ≥1.5-fold changes as cut-off values, did not show changes in expression on *Prdm14* induction in *Tet1*/*Tet2* DKD ESCs (Fig. 5B). Upregulation of the early PGC markers *Dppa3* and *Tcfap2c* by *Prdm14* induction did not depend on TET1/TET2 functions (Kurimoto et al., 2008b), whereas PRDM14-mediated upregulation of *Sycp1*, *Sycp3* and *Mael*, which are activated by TET1-dependent DNA demethylation in gonadal PGCs (Yamaguchi et al., 2012), does depend on TET1/TET2 functions. Systematic analysis of gene expression changes by qRT-PCR produced results that were consistent with microarray data (Fig. 5C). Next, to evaluate the effects of reduced TET1 and TET2 proteins on 5mC demethylation by PRDM14 overexpression, we monitored 5mC and 5hmC levels at target genes by GlucMS-qPCR. The 5hmC levels at the genes we analyzed were consistently low in *Tet1*/*2* DKD ESCs, which suggests that the functions of TET1 and TET2 were impaired in *Tet1*/*2* DKD ESCs (Fig. 5D, Fig. 8A). Consistent with the changes in expression, the reduction in 5mC levels at *Syce1*, *Slc25a31*, *Mael*, *Tdrd12*, *Mei1*, *Spo11* and *Igf2r* were significantly impaired by PRDM14 overexpression in a *Tet1*/*Tet2* DKD background. In the case of *Piwil2* and *Prss21*, 5mC levels were higher in *Tet1*/*Tet2* DKD ESCs compared with control ESCs, before *Prdm14* induction, and the 5mC levels on those genes were significantly decreased both in control ESCs and *Tet1*/*Tet2* DKD ESCs after *Prdm14* induction. These results suggest that PRDM14 promotes *Tet1*/*Tet2*-independent DNA demethylation on *Piwil2* and *Prss21*. In contrast to *Tet1*/*Tet2* DKO ESCs, we found a modest reduction in 5mC levels at these genes by PRDM14 overexpression in *Tet1* single knockdown (KD) ESCs, compared with that observed in the control ESCs (supplementary material Fig. S2). Overall, these results provide evidence that both TET1 and TET2 contribute to PRDM14-dependent DNA demethylation.

PRDM14 promotes active DNA demethylation through the BER pathway

To determine the mechanistic links between PRDM14 and the BER pathway in DNA demethylation, we used pharmacological inhibitors of the BER pathway and knockdown experiments for *Tdg* in PRDM14-dependent DNA demethylation. We first used pharmacological inhibitors of the BER components PARP1 (inhibitor: 3-aminobenzamide, 3AB) and APE1 (inhibitor: CRT0044876, CRT). Two inhibitors of the BER pathway severely impaired the upregulation of *Piwil2*, *Syce1*, *Slc25a31*, *Mael*, *Prss21*, *Tdrd12*, *Mei1* and *Spo11* after *Prdm14* induction (Fig. 6A). To investigate whether this observation correlated with changes in 5mC and 5hmC levels near the TSS of these genes, we monitored 5mC and 5hmC levels by GlucMS-qPCR. 5mC demethylation of *Piwil2*, *Syce1*, *Slc25a31*, *Mael*, *Igf2r*, *Prss21*, *Tdrd12*, *Mei1* and *Spo11* by PRDM14 overexpression was consistently disturbed in the presence of BER inhibitors (Fig. 6B, Fig. 8A). 5hmC and its further oxidized forms, 5-formylcytosine (5fC) and 5-carboxycytosine (5caC), can be removed through two pathways: BER-dependent active demethylation and replication-coupled passive demethylation (Guo et al., 2011; He et al., 2011; Ito et al., 2011). Our BER inhibitor experiments suggested the possibility that PRDM14-dependent DNA demethylation depends only on BER-mediated active mechanisms and not on passive mechanisms because ESCs exhibit highly proliferative activity. To verify this possibility, we investigated the involvement of DNA replication of ESCs in PRDM14-dependent DNA demethylation. We treated *Prdm14*-induced ESCs with aphidicolin, a pharmacological inhibitor of G1/S progression, from day 0 to day 1.5 with or without Dox (supplementary material Fig. S3). We found a significant reduction in 5mC at target loci of PRDM14-dependent demethylation after PRDM14 overexpression, despite the presence of aphidicolin (Fig. 6C). Based on the effects of BER inhibitors and aphidicolin in PRDM14-dependent 5mC demethylation, it can be concluded that PRDM14 overexpression removes the 5mC of the target genes through the BER pathway.

DNA demethylation by PRDM14 depends on TDG

It was previously assumed that 5hmC, produced by TET proteins, can be deaminated by AID or further oxidized by TET proteins to produce 5-hydroxymethyluracil (5hmU) or 5fC/5caC. 5hmU and 5fC/5caC might then be recognized and removed by DNA glycosylases, followed by BER (Guo et al., 2011). TDG has been shown to exhibit glycosylase activity for 5hmU and 5caC (Hashimoto et al., 2012). Therefore, to investigate whether TDG is the glycosylase responsible for BER in active demethylation caused by PRDM14 overexpression, we depleted *Tdg* in ESCs carrying doxycycline-inducible *Prdm14* expression units (Fig. 7A). The repression of TDG functions impaired upregulation of *Piwil2*, *Slc25a31*, *Mael*, *Prss21*, *Tdrd12*, *Mei1* and *Spo11* but not *Syce1* after Prdm14 induction (Fig. 7B). Consistent with the impairment of transcriptional activation by PRDM14 in *Tdg* KD ESCs, we found that the depletion of *Tdg* impaired 5mC reduction at the *Piwil2*, *Slc25a31*, *Mael*, *Igf2r*, *Prss21*, *Tdrd12*, *Mei1* and *Spo11* but not *Syce1* differentially methylated regions (DMRs) by PRDM14 overexpression (Fig. 7C, Fig. 8A). Furthermore, we observed consistent elevation of 5hmC at those regions after *Prdm14* induction in *Tdg* KD ESCs, implying that the removal of 5hmC by TDG regions was impaired (Fig. 7C, Fig. 8B). Next, we monitored the enrichment of APE1 and TDG at *Slc25a31*, *Piwil2*, *Vmn2r29* and *Sfi1* after *Prdm14* induction by ChIP analysis. We found transient elevation of the enrichment of APE1 and TDG at *Slc25a31* and *Piwil2*, but not at *Vmn2r29* and *Sfi1* (Fig. 7D). Our cumulative data provide evidence that PRDM14 promotes active DNA demethylation through the TET-mediated BER in cooperation with the repression of *Dnmt3b* and *Dnmt3l* (Fig. 8C).

DISCUSSION

Here, we have provided evidence that PRDM14 induces DNA demethylation at pluripotency-associated genes, germline-specific genes and imprinted loci, but not across the entire genome, through the TET-mediated BER pathway. Several recent studies have suggested that 5hmC is converted to cytosine by the action of several independent passive or active pathways, which may operate in parallel (Hackett et al., 2012b). Our data show that the repression of TET functions and the BER pathway significantly impairs DNA demethylation induced by PRDM14 in ESCs, despite the observation that ESCs are highly proliferative. Furthermore, DNA demethylation by PRDM14 effectively takes place in the presence of aphidicolin, which is a pharmacological inhibitor of G1/S progression. Cumulative data have provided evidence that replication-dependent passive demethylation does not participate in PRDM14-dependent DNA demethylation.

Our data clearly provide evidence that PRDM14-dependent demethylation strongly depends on TET1 and TET2 function in ESCs. *Prdm14* is crucial for ESC derivation in the presence of LIF-containing serum, whereas *Prdm14* KO ESCs can be expanded in the presence of LIF-containing 2i medium (Grabole et al., 2013;

Development (2014) doi:10.1242/dev.099622

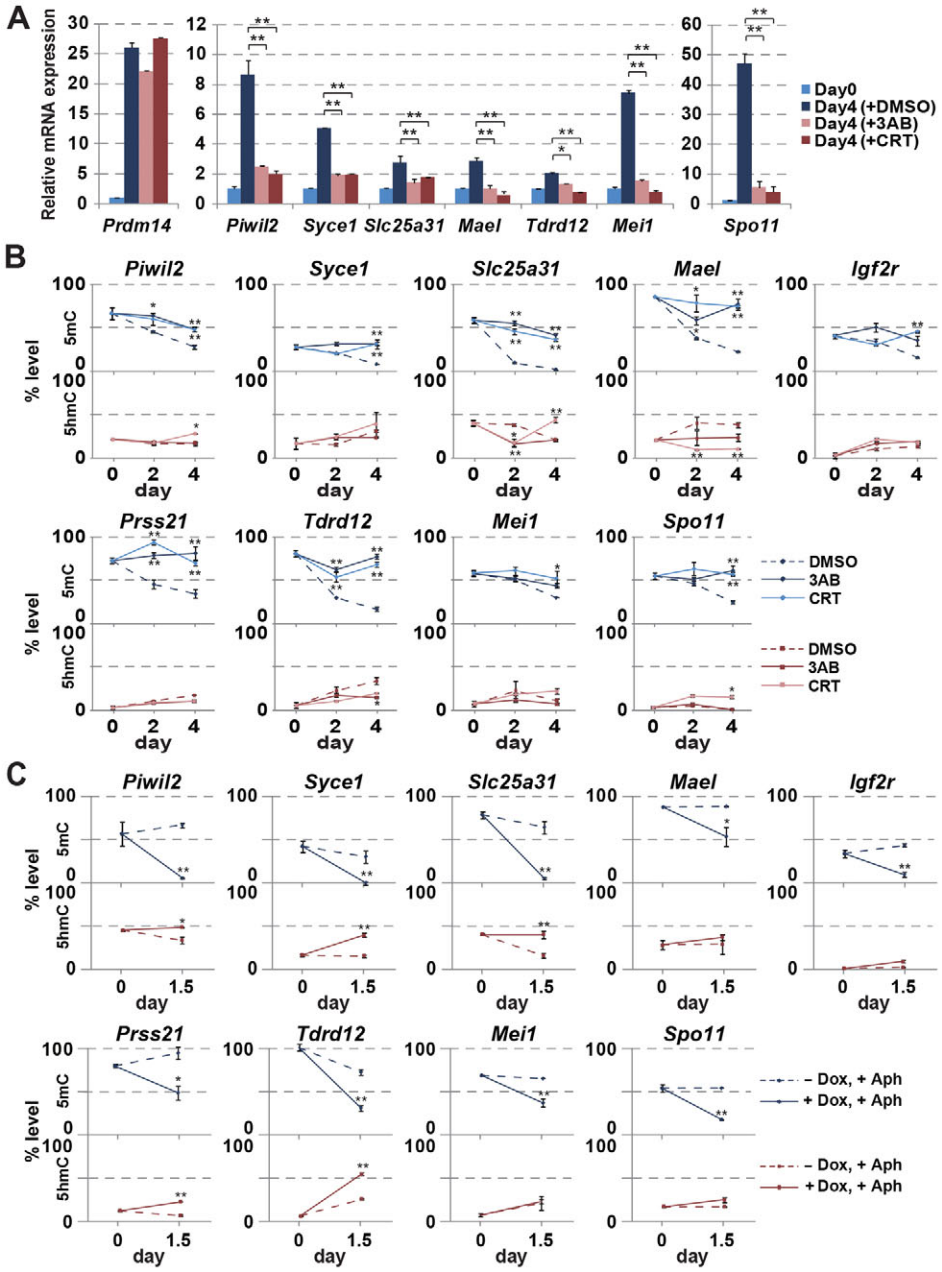

Fig. 6. PRDM14-dependent DNA demethylation depends on BER but not on DNA replication. (A) qRT-PCR analysis of *Prdm14*, *Piwil2*, *Syce1*, *Slc25a31*, *Mael*, *Prss21*, *Tdrd12*, *Mei1* and *Spo11* in *Prdm14*-inducible ESCs with DMSO as the vehicle control or 3AB or CRT after *Prdm14* induction. (B) GlucMS-qPCR analysis of 5mC and 5hmC at or near the TSS of *Piwil2*, *Syce1*, *Slc25a31*, *Mael*, *Igf2r*, *Prss21*, *Tdrd12*, *Mei1* and *Spo11* in *Prdm14*-inducible ESCs with DMSO as the vehicle control or 3AB or CRT after *Prdm14* induction. (C) GlucMS-qPCR analysis of 5mC and 5hmC at or near the TSS of *Piwil2*, *Syce1*, *Slc25a31*, *Mael*, *Igf2r*, *Prss21*, *Tdrd12*, *Mei1* and *Spo11* in *Prdm14*-inducible ESCs with aphidicolin after *Prdm14* induction. Error bars indicate the s.e.m. values of technical duplicates of qPCR results. *P* values for qRT-PCR and GlucMS-qPCR were obtained using Student's *t*-test. **P*<0.05, ***P*<0.01.

Yamaji et al., 2013). *Prdm14* KO ESCs normally expressed OCT4 (POU5F1 – Mouse Genome Informatics), SOX2 and NANOG at levels similar to those in wild-type ESCs. However, DNA methylation levels on *Tcl1* and germline-specific genes are significantly elevated in *Prdm14* KO ESCs in the presence of LIF-containing 2i medium, which is consistent with results from our current study (Yamaji et al., 2013). In *Prdm14* KO ESCs, the expression of *de novo* DNA methyltransferases *Dnmt3a*, *Dnmt3b* and *Dnmt3l* are significantly upregulated, which contributes to the aberrant hypermethylation on pluripotency-associated and germline-specific genes (Grabole et al., 2013; Leitch et al., 2013; Yamaji et al., 2013). Our data indicated that PRDM14 overexpression represses *Dnmt3b* and *Dnmt3l* but not *Dnmt3a*. By contrast, substantial downregulation of *Dnmt3a*, *Dnmt3b* and *Dnmt3l* in ESCs was observed in the process of switching from LIF-containing serum to LIF-containing 2i medium associated with the elevation of *Prdm14* expression. These findings suggest that an additional mechanism with the elevation of PRDM14 is required for the downregulation of *Dnmt3a* in LIF-containing 2i medium. In contrast to *Prdm14* KO ESCs, *Tet1*/*Tet2* DKO ESCs have self-renewal capacity in the presence of LIF-containing serum (Dawlaty et al., 2013). However, acute depletion of *Tet1* by siRNA reduces the expressions of pluripotency-associated genes associated with the elevation of 5mC on those genes (Ficz et al., 2011; Ito et al., 2010). Furthermore, a recent study has shown that TET1/TET2-mediated conversion from 5mC to 5hmC followed by passive demethylation is involved in global hypomethylation in naive pluripotent stem cells (Ficz et al., 2013). Considering the results from both previous studies and our current study, we propose that the TET-mediated BER pathway promoted by PRDM14 cooperates with TET-mediated passive demethylation and repression of *Dnmt3a*/*b*/*l* to sustain global hypomethylation in the ICM and naive pluripotent stem cells. Further studies are required to clarify whether endogenous PRDM14 accelerates the TET-BER cycle for active

Development (2014) doi:10.1242/dev.099622

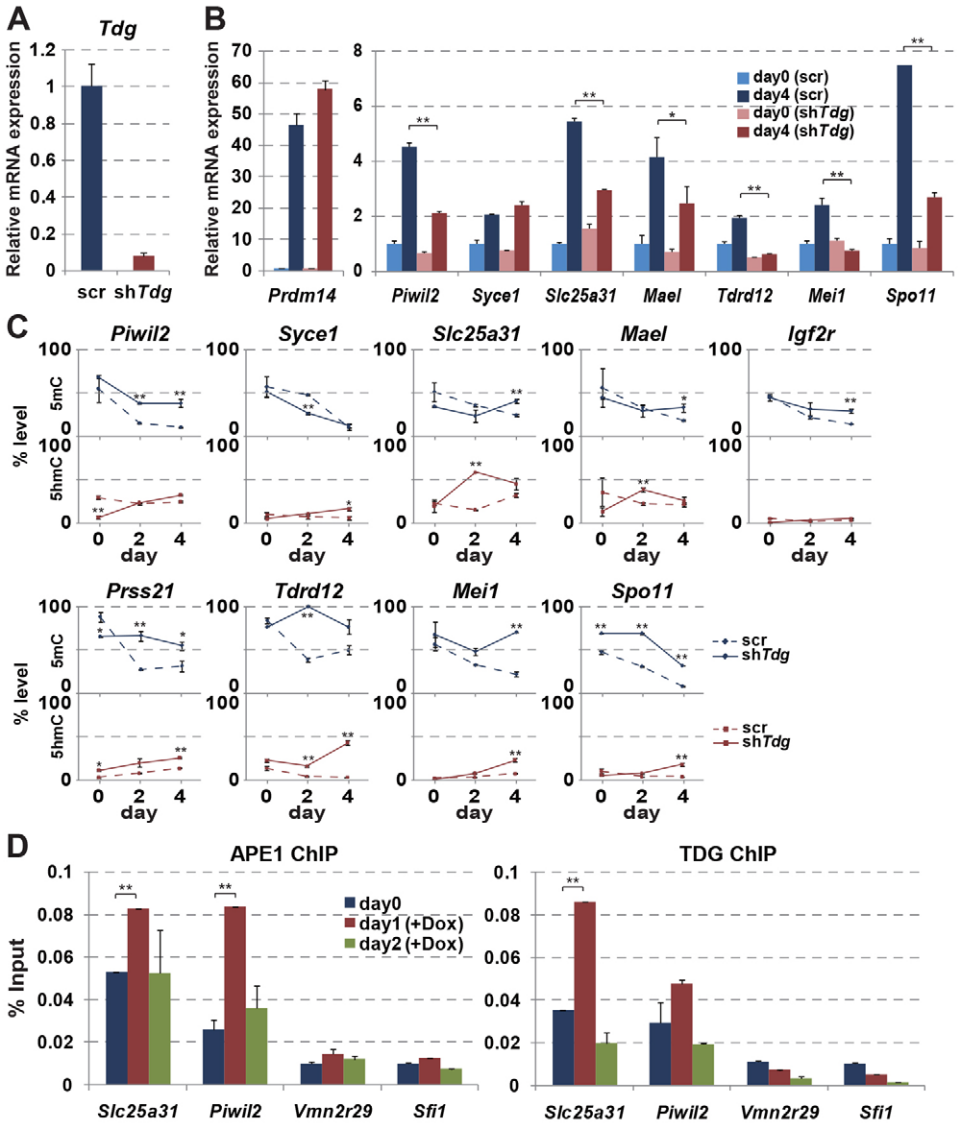

Fig. 7. PRDM14-dependent DNA demethylation is impaired by TDG reduction. (A) Knockdown efficiency was validated by qRT-PCR for *Tdg*. (B) qRT-PCR analysis of *Prdm14*, *Piwil2*, *Syce1*, *Slc25a31*, *Mael*, *Prss21*, *Tdrd12*, *Mei1* and *Spo11* in *Prdm14*-inducible ESCs with scrambled shRNA and *Tdg* shRNA after *Prdm14* induction. (C) GlucMS-qPCR analysis of 5mC and 5hmC at or near the TSS of *Piwil2*, *Syce1*, *Slc25a31*, *Mael*, *Igf2r*, *Prss21*, *Tdrd12*, *Mei1* and *Spo11* in *Prdm14*-inducible ESCs with scrambled shRNA and *Tdg* shRNA after *Prdm14* induction. (D) ChIP analysis of APE1 and TDG at or near the TSS of *Slc25a31*, *Piwil2*, *Vmn2r29* and *Sfi1* in *Prdm14*-inducible ESCs with or without Dox. Error bars indicate the s.e.m. values of technical duplicates of qPCR results. *P* values for qRT-PCR, GlucMS-qPCR and ChIP-qPCR were obtained using Student's *t*-test. **P*<0.05, ***P*<0.01.

DNA demethylation in naive ESCs. Interestingly, CpG methylation at imprinted differentially methylated regions was maintained in ESCs in the presence of LIF-containing 2i medium associated with the elevation of *Prdm14* expression (Leitch et al., 2013). By contrast, our gain-of-function experiments indicated that PRDM14 promotes active DNA demethylation at pluripotency-associated genes, germline-specific genes and imprinted loci. We have shown that the expression level of *Prdm14* is low in the ICM and naive pluripotent stem cells, whereas developing PGCs show high expression of *Prdm14* (Yamaji et al., 2008), which might be responsible for the difference in sensitivity against PRDM14-dependent active demethylation at imprinted loci. Consistent with this hypothesis, the transcript level of *Prdm14* in our overexpression system in ESCs was found to be similar to that in developing PGCs but not that in naive ESCs (supplementary material Fig. S1A). Further detailed studies are required to determine whether PRDM14-dependent active DNA demethylation is involved in the erasure of genomic imprinting.

Our comparisons of the global gene expression profiles of PRDM14-overexpressing ESCs obtained with scrambled shRNA and those obtained with *Tet1*/*Tet2* shRNA, performed by microarray analysis, showed that both transcriptional activation and repression by PRDM14 overexpression significantly depends on TET1 and TET2 functions. Interestingly, PRDM14 upregulation of the early PGC markers *Dppa3* and *Tcfap2c* normally occurs in ESCs with a *Tet1*/*Tet2* DKD background (Kurimoto et al., 2008a), whereas PRDM14-dependent upregulation of the late PGC markers *Sycp1*, *Sycp3*, *Mael* and *Hormad1* is significantly disrupted by the repression of TET1 and TET2 functions in ESCs associated with the impairment of DNA demethylation by PRDM14. Our data are consistent with both *Tet1* and *Tet1*/*Tet2* KO mice phenotypes (Dawlaty et al., 2013; Yamaguchi et al., 2012). In both *Tet1* and *Tet1*/*Tet2* KO mice, it has been demonstrated that PGC specification and early differentiation associated with the activation of early PGC markers, including *Dppa3* and *Tcfap2c*, occurs normally. However, *Tet1*-deficient female mice exhibited subfertility associated with the failure of meiotic entry in gonadal PGCs. *Tet1* deficiency leads to defective DNA demethylation and decreased expression of early meiotic genes, including *Sycp1*, *Sycp3*, *Mael* and *Hormad1*. These findings raise the possibility that TET-BER-mediated active DNA demethylation promoted by PRDM14 is required for locus-specific DNA demethylation to ensure proper entry into meiosis for gonadal PGCs. Our microarray data suggest that TET1 and TET2 play crucial roles for not only DNA demethylation but also

Development (2014) doi:10.1242/dev.099622

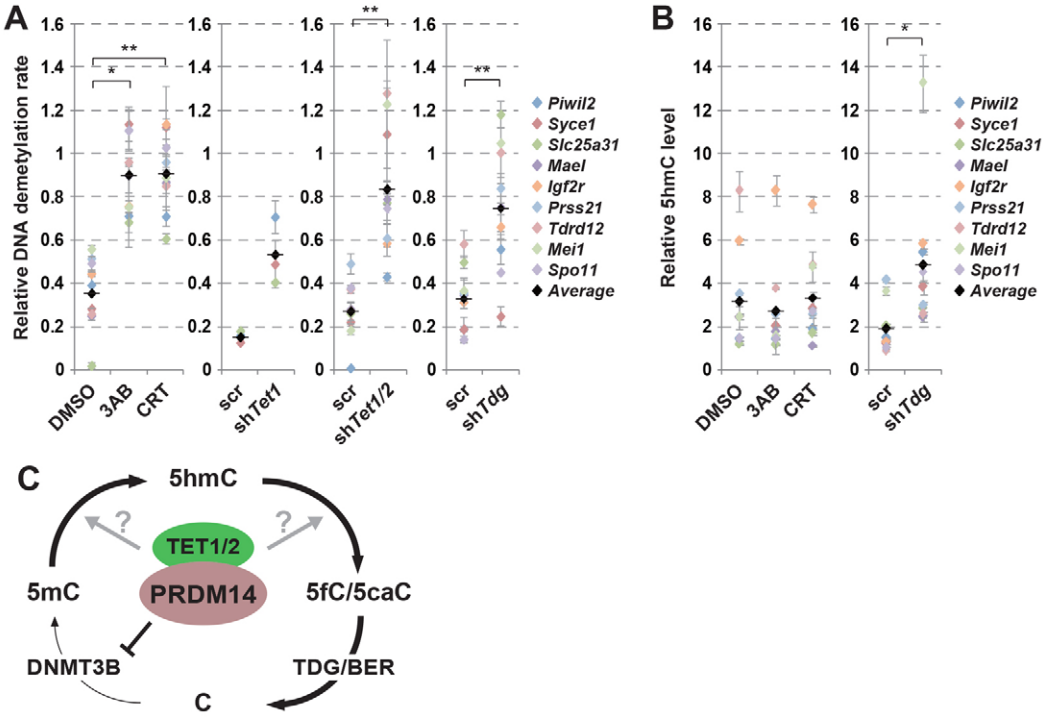

Fig. 8. A schematic for active DNA demethylation by PRDM14. (A,B) Relative 5mC and 5hmC levels at target loci. The methylation percentage of individual target loci in ESCs without Dox in each condition was set as 1. Colored dots indicate relative methylation levels around the TSS of individual genes. Black dots indicate the average of relative methylation levels around the TSS of individual genes. *P* values were obtained using Student's *t*-test. **P*<0.05, ***P*<0.01. (C) A schematic for the acceleration of the TET-BER cycle by PRDM14.

transcriptional repression by PRDM14. The evidence also indicates that TET1 plays a role in transcriptional regulation by cooperating with polycomb repressive complex 2 (PRC2) and the SIN3A co-repressor complex (Williams et al., 2011; Wu et al., 2011). Interestingly, PRDM14 represses gene expression by recruiting PRC2 but not SIN3A in ESCs (Yamaji et al., 2013). These cumulative findings suggest that PRDM14 forms a complex with TET1/2 and PRC2 to act as a transcriptional repressor in ESCs.

5hmC produced by TET-mediated oxidation of 5mC is further catalyzed by two independent pathways: 5hmC is further oxidized to produce 5fC/5caC by TET proteins (He et al., 2011; Ito et al., 2011) or 5hmC is deaminated to produce 5hmU by AID/Apobec (Guo et al., 2011). 5fC/5caC and 5hmU are subsequently repaired by the TDG-mediated BER pathway (Cortellino et al., 2011; Guo et al., 2011; Shen et al., 2013; Song et al., 2013). Recent global profiling analyses of 5fC/5caC have shown that the loss of TDG leads to accumulation of 5fC/5caC but not 5hmC, which indicates that the majority of 5fC/5caC is in intermediate forms in the process of BER-mediated active demethylation in ESCs (Shen et al., 2013; Song et al., 2013). During our GlucMS-qPCR analysis, we observed the enrichment of the *Msp*I-resistant fraction at the target genes of PRDM14 after PRDM14 induction in ESCs in *Tdg* KD ESCs. Although 5hmC, 5hmU and 5fC/5caC may be present in the *Msp*I-resistant fraction, as shown by the results of GlucMS-qPCR analysis, we did not identify the forms that were enriched in the *Msp*I-resistant fraction in this study. Therefore, further investigation is required to identify the precise routes from 5hmC to unmodified cytosine during active demethylation by PRDM14. The 5fC/5caC content is very low compared with the 5hmC content in the mouse genome of ESCs, which suggests that oxidation from 5hmC to 5fC/5caC is tightly regulated and is less efficient than oxidation from 5mC to 5hmC (He et al., 2011; Ito et al., 2011). It is interesting to note that although the conversions from 5mC to 5hmC and from 5hmC to 5fC/5caC are regulated by the same enzymes (i.e. TETs), the mechanism associated with TET function remains poorly understood. A real-time system that can be used for monitoring the TET-BER cycle and which allows for the elucidation of the molecular mechanism regulating TET activity in each step of the 5mC oxidations is required. It is possible that our *Prdm14*-inducible system in ESCs could be used to monitor the temporal dynamics of TET-mediated 5mC oxidation, which might contribute to the elucidation of the regulation of 5mC oxidation by TET proteins.

Our study provides evidence that PRDM14 promotes TET-BER-mediated active DNA demethylation. Aberrant DNA methylation patterns of induced pluripotent stem cells (iPSCs), including hypermethylation of imprinted loci and retention of DNA methylation patterns of original cells, compromise the efficient differentiation capacity of iPSCs equivalent to that of ESCs (Ohi et al., 2011; Stadtfeld et al., 2010). We consider that active DNA demethylation by PRDM14 might contribute to the erasure of aberrant DNA methylation patterns in iPSCs.

MATERIALS AND METHODS

Cell culture, RNA extraction and qRT-PCR

J1 mouse ESCs were cultured under feeder-free conditions in Glasgow minimum essential medium (GMEM) (Wako) containing 10% fetal calf serum (Invitrogen), 1 mM glutamine (Wako), nonessential amino acid (Wako) and 0.1 mM 2-mercaptoethanol (Wako), and were supplemented with LIF (Wako). ESCs with doxycycline-inducible *Prdm14* expression were established by transfecting PB-TET-Flag-Prdm14-IRES-Neo, PB-CA-rtTA Adv, pCAG-Pbase and pGG131 (pCAG-DsRed-IRES-Hygro) into ESCs using Hilymax (DOJINDO), followed by selection with 200 µg/ml hygromycin B (WAKO) for 7 days (Guo et al., 2009; Wang et al., 2008; Woltjen et al., 2009). *Tet1*, *Tet2* and *Tdg* shRNAs were generated in pLKO.1-puro (Addgene, 8453) or pLKO.1-blast (Addgene, 26655). The

RNAi target sequences are provided in supplementary material Table S1. pLKO.1 lentiviruses were constructed using standard methods. pLKO.1 plasmids were co-transfected with pCMV-VSV-G (Addgene, 8454) and pCMV-dR8.2 dvpr (Addgene, 8455) into HEK293T cells. For lentivirus transduction, subconfluent cultured iP14 ESCs were incubated with lentivirus-containing Dulbecco's modified Eagle's medium (DMEM) supplemented with 8 µg/ml Polybrene (Sigma-Aldrich) for 24 hours. After exchanging the medium with fresh medium, cells were selected with 2 µg/ml puromycin or 20 µg/ml blasticidin S hydrochloride (Calbiochem). Knockdown efficiency was analyzed by performing qRT-PCR and western blotting. Total RNA was extracted using TRIzol (Invitrogen) and the ReverTra Ace qPCR RT kit (Toyobo) was used for cDNA synthesis, according to the manufacturer's instructions. Subsequently, cDNA was used as a template for qPCR performed with the Thermal Cycler Dice Real Time System (Takara) and Thunderbird SYBR qPCR Mix (TOYOBO) with gene-specific primers (supplementary material Table S1).

Western blotting, immunoprecipitation analyses and ChIP analysis

Cells were lysed by boiling in SDS sample buffer (Wako). Before lysed proteins were applied to polyacrylamide-SDS gels, 2-mercaptoethanol was added to denature the proteins. The lysed proteins were separated on polyacrylamide-SDS gels, blotted on a polyvinylidene fluoride membrane, and probed using the following primary antibodies: anti-histone H3 (Abcam, ab1791, 1:2500), anti-FLAG (Sigma, F1804, 1:500), anti-TET1 (Millipore, 09-872, 1:500) and anti-TET2 (Santa Cruz, sc-136926, 1:500). Following the primary antibody reaction, the membrane was incubated with secondary horseradish peroxidase-coupled antibodies (Santa Cruz; mouse, sc-2005, 1:2500; rabbit, sc-2004, 1:2500). Detection was performed using the Luminata Forte Western HRP Substrate (Millipore). For immunoprecipitation analysis, nuclear extracts containing a protease-inhibitor cocktail (Maison et al., 2002) were incubated with anti-PRDM14 antibody (1:1000) (Yamaji et al., 2008) at 4°C overnight and captured with protein A beads. Protein complexes were washed with wash buffer (20 mM HEPES, pH 7.6, 1.5 mM $MgCl_2$, 150 mM NaCl, 0.2 mM EDTA, 0.5 mM DTT and 20% glycerol) and eluted by boiling with SDS sample buffer. ChIP analyses were performed as previously described (Ohno et al., 2013).

DNA methylation analysis

Genomic DNA was isolated using the Wizard SV Genomic DNA Purification System (Promega). For Gluc-MS-qPCR analysis, genomic DNA (2250 ng) was treated with T4 phage β-glucosyltransferase (T4-BGT, NEB M0357S), according to the manufacturer's instructions. Glycosylated genomic DNA (750 ng) was digested with 40 U of either *Hpa*II or *Msp*I, or no enzyme, at 37°C overnight, followed by inactivation by proteinase K treatment. The *Hpa*II- or *Msp*I-resistant fractions were quantified by qPCR using primers designed around a single *Hpa*II/*Msp*I site and normalized to the region lacking *Hpa*II/*Msp*I sites. Resistance to *Msp*I directly translated to the percentage of 5hmC, whereas the percentage of 5mC was calculated by subtracting the 5hmC contribution from the total *Hpa*II resistance. Bisulphite sequencing was carried out with the Episight Bisulfite Conversion Kit (WAKO). MeDIP was performed using 4 µg of heat-denatured, sonicated DNA and 10 µg of 5-methylcytidine antibody (Eurogentec/Anaspec #BI-MECY-0500). Briefly, 4 mg of sheared input DNA was diluted into 450 µl of TE buffer (10 mM Tris-HCl pH 8, 1 mM EDTA). DNA was denatured for 10 minutes at 100°C in a dry heat block and then immediately placed on ice for 5-10 minutes in 51 µl of IP buffer (100 mM sodium-phosphate, pH 7.0, 1.4 M NaCl and 0.5% Triton X-100), followed by addition of 10 µg of 5-methylcytidine antibody (BIMECY-0500; Eurogentec) or 10 µg of normal mouse IgG (Millipore). Immunoprecipitation (IP) was performed at 4°C with rotation for 2 hours. Antibody-DNA complexes were pulled down by adding 40 µl of Dynabeads (M-280) sheep anti-mouse IgG (Invitrogen) directly to the IP reaction at 4°C for 2 hours with rotation. Beads were collected with a 1.5-ml microcentrifuge tube holder magnet and washed three times in IP buffer at room temperature (10 minutes per wash with rotation). The washed beads were collected with a magnet and resuspended in 250 µl of proteinase K digestion buffer (50 mM Tris pH 8.0, 10 mM EDTA and 0.5% SDS). Then, 3.5 µl of 20 mg/ml proteinase K was added, and digestion was performed at 50°C for 3 hours in a thermomixer (Eppendorf) set at 800 rpm (72 ***g***). Beads were collected with a magnet, and DNA was extracted from the supernatant first with phenol and then with chloroform. DNA was precipitated with 400 mM NaCl, 15 µg linear acrylamide and two volumes of 100% ethanol at 35°C overnight. The precipitated DNA was resuspended in 11 µl of nuclease-free H_2O, and the DNA concentrations were determined using a NanoDrop spectrophotometer. Then, 25-40 ng of input genomic DNA or 5-mC-IPed DNA was used. DNA fragments of ~150-300 bp were gel-purified after the adaptor ligation step. PCR-amplified DNA libraries were quantified on an Agilent 2100 Bioanalyzer and diluted to 6-8 pM for cluster generation and sequencing. Then, 100-cycle paired-end sequencing was performed using the Illumina HiSeq2000 system. In addition to our MeDIP-seq datasets, PRDM14 ChIP-seq datasets (Ma et al., 2011) were downloaded from the Gene Expression Omnibus database (GSE25409). Paired mapping of MeDIP-seq datasets to the mouse genome (NCBI build 37/mm9) was performed using Bowtie2 v2.0.2 (Langmead and Salzberg, 2012) with the 'X 1000–no-mixed–no-discordant–sensitive' options. Unpaired mapping of PRDM14 ChIP-seq datasets was performed using the 'sensitive' option. In order to exclude PCR amplification artifacts from the mapped reads, multiple reads were removed by the 'rmdup' command of SAMtools v0.1.18 (Li et al., 2009). The mapped reads were visualized using the Integrative Genomics Viewer (IGV) v2.2 (Thorvaldsdóttir et al., 2013). LC-MS/MS analysis of genomic DNA was performed as previously described (Spruijt et al., 2013).

Microarray expression analysis

Total RNA from control and *Tet1*/*Tet2* double knockdown (sh*Tet1*/*Tet2*) iP14 ESCs (± Dox) was purified using the PureLink RNA Mini Kit (Ambion). Total RNA (150 ng) was labeled using a GeneChip 3′ IVT Express Kit (Affymetrix) and hybridized to an Affymetrix MG-430 pm array strip performed on the GeneAtlas system (Affymetrix), according to the manufacturer's instructions. The microarray data were quantile-normalized and analyzed using custom R scripts with the limma package (Smyth et al., 2005). Microarray data are available at GEO with accession number GSE52598.

Inhibition of the base excision repair pathway

Prdm14 expression was induced by treatment with 1 µg/ml Dox. Concomitant with the induction of PRDM14, a small molecule inhibitor of the base excision repair pathway, either 5 mM 3-AB (Sigma-Aldrich) or 100 µM CRT0044876 (Calbiochem) in 0.1% DMSO, was added to the medium.

Acknowledgements

We thank G. Nagamatsu for technical advice, K. Nishiwaki for encouragement and support, and M. Saitou for providing the *Prdm14* KO ESCs.

Competing interests

The authors declare no competing financial interests.

Author contributions

N.O., K.E. and M. Nishi established the cell lines and performed the DNA methylation, qRT-PCR, and microarray analyses. Y.K. performed the bioinformatics analysis of MeDIP-Seq. Y.O., N.K. and T.T. performed LC-MS/MS. S.H. performed bioinformatics analysis of the microarray data. M. Nakayama established the *Tdg* KD ESCs. T.N. and K.S. generated TDG antibody. M.O. provided advice regarding writing of the manuscript. Y.S. designed the experiments and wrote the manuscript.

Funding

This study was supported by JSPS KAKENHI grant number 24681040; by the Takeda Science foundation; by the Sumitomo foundation; by the Chemicals Evaluation and Research Institute; and by an Individual Special Research A grant from Kwansei Gakuin University.

Supplementary material

Supplementary material available online at
http://dev.biologists.org/lookup/suppl/doi:10.1242/dev.099622/-/DC1

References

Cortellino, S., Xu, J., Sannai, M., Moore, R., Caretti, E., Cigliano, A., Le Coz, M., Devarajan, K., Wessels, A., Soprano, D. et al. (2011). Thymine DNA glycosylase is

essential for active DNA demethylation by linked deamination-base excision repair. *Cell* **146**, 67-79.

Dawlaty, M. M., Breiling, A., Le, T., Raddatz, G., Barrasa, M. I., Cheng, A. W., Gao, Q., Powell, B. E., Li, Z., Xu, M. et al. (2013). Combined deficiency of Tet1 and Tet2 causes epigenetic abnormalities but is compatible with postnatal development. *Dev. Cell* **24**, 310-323.

Ficz, G., Branco, M. R., Seisenberger, S., Santos, F., Krueger, F., Hore, T. A., Marques, C. J., Andrews, S. and Reik, W. (2011). Dynamic regulation of 5-hydroxymethylcytosine in mouse ES cells and during differentiation. *Nature* **473**, 398-402.

Ficz, G., Hore, T. A., Santos, F., Lee, H. J., Dean, W., Arand, J., Krueger, F., Oxley, D., Paul, Y. L., Walter, J. et al. (2013). FGF signaling inhibition in ESCs drives rapid genome-wide demethylation to the epigenetic ground state of pluripotency. *Cell Stem Cell* **13**, 351-359.

Grabole, N., Tischler, J., Hackett, J. A., Kim, S., Tang, F., Leitch, H. G., Magnúsdóttir, E. and Surani, M. A. (2013). Prdm14 promotes germline fate and naive pluripotency by repressing FGF signalling and DNA methylation. *EMBO Rep.* **14**, 629-637.

Guibert, S., Forné, T. and Weber, M. (2012). Global profiling of DNA methylation erasure in mouse primordial germ cells. *Genome Res.* **22**, 633-641.

Guo, G., Yang, J., Nichols, J., Hall, J. S., Eyres, I., Mansfield, W. and Smith, A. (2009). Klf4 reverts developmentally programmed restriction of ground state pluripotency. *Development* **136**, 1063-1069.

Guo, J. U., Su, Y., Zhong, C., Ming, G. L. and Song, H. (2011). Hydroxylation of 5-methylcytosine by TET1 promotes active DNA demethylation in the adult brain. *Cell* **145**, 423-434.

Hackett, J. A., Sengupta, R., Zylicz, J. J., Murakami, K., Lee, C., Down, T. A. and Surani, M. A. (2012a). Germline DNA demethylation dynamics and imprint erasure through 5-Hydroxymethylcytosine. *Science* **339**, 448-452.

Hackett, J. A., Zylicz, J. J. and Surani, M. A. (2012b). Parallel mechanisms of epigenetic reprogramming in the germline. *Trends Genet.* **28**, 164-174.

Hashimoto, H., Hong, S., Bhagwat, A. S., Zhang, X. and Cheng, X. (2012). Excision of 5-hydroxymethyluracil and 5-carboxylcytosine by the thymine DNA glycosylase domain: its structural basis and implications for active DNA demethylation. *Nucleic Acids Res.* **40**, 10203-10214.

He, Y. F., Li, B. Z., Li, Z., Liu, P., Wang, Y., Tang, Q., Ding, J., Jia, Y., Chen, Z., Li, L. et al. (2011). Tet-mediated formation of 5-carboxylcytosine and its excision by TDG in mammalian DNA. *Science* **333**, 1303-1307.

Ito, S., D'Alessio, A. C., Taranova, O. V., Hong, K., Sowers, L. C. and Zhang, Y. (2010). Role of Tet proteins in 5mC to 5hmC conversion, ES-cell self-renewal and inner cell mass specification. *Nature* **466**, 1129-1133.

Ito, S., Shen, L., Dai, Q., Wu, S. C., Collins, L. B., Swenberg, J. A., He, C. and Zhang, Y. (2011). Tet proteins can convert 5-methylcytosine to 5-formylcytosine and 5-carboxylcytosine. *Science* **333**, 1300-1303.

Kagiwada, S., Kurimoto, K., Hirota, T., Yamaji, M. and Saitou, M. (2013). Replication-coupled passive DNA demethylation for the erasure of genome imprints in mice. *EMBO J.* **32**, 340-353.

Kurimoto, K., Yabuta, Y., Ohinata, Y., Shigeta, M., Yamanaka, K. and Saitou, M. (2008a). Complex genome-wide transcription dynamics orchestrated by Blimp1 for the specification of the germ cell lineage in mice. *Genes Dev.* **22**, 1617-1635.

Kurimoto, K., Yamaji, M., Seki, Y. and Saitou, M. (2008b). Specification of the germ cell lineage in mice: a process orchestrated by the PR-domain proteins, Blimp1 and Prdm14. *Cell Cycle* **7**, 3514-3518.

Langmead, B. and Salzberg, S. L. (2012). Fast gapped-read alignment with Bowtie 2. *Nat. Methods* **9**, 357-359.

Leitch, H. G., McEwen, K. R., Turp, A., Encheva, V., Carroll, T., Grabole, N., Mansfield, W., Nashun, B., Knezovich, J. G., Smith, A. et al. (2013). Naive pluripotency is associated with global DNA hypomethylation. *Nat. Struct. Mol. Biol.* **20**, 311-316.

Li, E., Bestor, T. H. and Jaenisch, R. (1992). Targeted mutation of the DNA methyltransferase gene results in embryonic lethality. *Cell* **69**, 915-926.

Li, H., Handsaker, B., Wysoker, A., Fennell, T., Ruan, J., Homer, N., Marth, G., Abecasis, G., Durbin, R.; 1000 Genome Project Data Processing Subgroup (2009). The Sequence Alignment/Map format and SAMtools. *Bioinformatics* **25**, 2078-2079.

Ma, Z., Swigut, T., Valouev, A., Rada-Iglesias, A. and Wysocka, J. (2011). Sequence-specific regulator Prdm14 safeguards mouse ESCs from entering extraembryonic endoderm fates. *Nat. Struct. Mol. Biol.* **18**, 120-127.

Maison, C., Bailly, D., Peters, A. H., Quivy, J. P., Roche, D., Taddei, A., Lachner, M., Jenuwein, T. and Almouzni, G. (2002). Higher-order structure in pericentric heterochromatin involves a distinct pattern of histone modification and an RNA component. *Nat. Genet.* **30**, 329-334.

Marks, H., Kalkan, T., Menafra, R., Denissov, S., Jones, K., Hofemeister, H., Nichols, J., Kranz, A., Stewart, A. F., Smith, A. et al. (2012). The transcriptional and epigenomic foundations of ground state pluripotency. *Cell* **149**, 590-604.

Nabel, C. S., Jia, H., Ye, Y., Shen, L., Goldschmidt, H. L., Stivers, J. T., Zhang, Y. and Kohli, R. M. (2012). AID/APOBEC deaminases disfavor modified cytosines implicated in DNA demethylation. *Nat. Chem. Biol.* **8**, 751-758.

Ohi, Y., Qin, H., Hong, C., Blouin, L., Polo, J. M., Guo, T., Qi, Z., Downey, S. L., Manos, P. D., Rossi, D. J. et al. (2011). Incomplete DNA methylation underlies a transcriptional memory of somatic cells in human iPS cells. *Nat. Cell Biol.* **13**, 541-549.

Ohinata, Y., Payer, B., O'Carroll, D., Ancelin, K., Ono, Y., Sano, M., Barton, S. C., Obukhanych, T., Nussenzweig, M., Tarakhovsky, A. et al. (2005). Blimp1 is a critical determinant of the germ cell lineage in mice. *Nature* **436**, 207-213.

Ohno, R., Nakayama, M., Naruse, C., Okashita, N., Takano, O., Tachibana, M., Asano, M., Saitou, M. and Seki, Y. (2013). A replication-dependent passive mechanism modulates DNA demethylation in mouse primordial germ cells. *Development* **140**, 2892-2903.

Okano, M., Bell, D. W., Haber, D. A. and Li, E. (1999). DNA methyltransferases Dnmt3a and Dnmt3b are essential for de novo methylation and mammalian development. *Cell* **99**, 247-257.

Seisenberger, S., Andrews, S., Krueger, F., Arand, J., Walter, J., Santos, F., Popp, C., Thienpont, B., Dean, W. and Reik, W. (2012). The dynamics of genome-wide DNA methylation reprogramming in mouse primordial germ cells. *Mol. Cell* **48**, 849-862.

Seki, Y., Hayashi, K., Itoh, K., Mizugaki, M., Saitou, M. and Matsui, Y. (2005). Extensive and orderly reprogramming of genome-wide chromatin modifications associated with specification and early development of germ cells in mice. *Dev. Biol.* **278**, 440-458.

Seki, Y., Yamaji, M., Yabuta, Y., Sano, M., Shigeta, M., Matsui, Y., Saga, Y., Tachibana, M., Shinkai, Y. and Saitou, M. (2007). Cellular dynamics associated with the genome-wide epigenetic reprogramming in migrating primordial germ cells in mice. *Development* **134**, 2627-2638.

Sharif, J., Muto, M., Takebayashi, S., Suetake, I., Iwamatsu, A., Endo, T. A., Shinga, J., Mizutani-Koseki, Y., Toyoda, T., Okamura, K. et al. (2007). The SRA protein Np95 mediates epigenetic inheritance by recruiting Dnmt1 to methylated DNA. *Nature* **450**, 908-912.

Shen, L., Wu, H., Diep, D., Yamaguchi, S., D'Alessio, A. C., Fung, H. L., Zhang, K. and Zhang, Y. (2013). Genome-wide analysis reveals TET- and TDG-dependent 5-methylcytosine oxidation dynamics. *Cell* **153**, 692-706.

Smyth, G., Gentleman, R., Carey, V. J., Huber, W., Irizarry, R. A. and Dudoit, S. (2005). *limma: Linear Models for Microarray Data Bioinformatics and Computational Biology Solutions Using R and Bioconductor* (ed. M. Gail, J. M. Samet, A. Tsiatis and W. Wong), pp. 397-420. New York, NY: Springer.

Song, C. X., Szulwach, K. E., Dai, Q., Fu, Y., Mao, S. Q., Lin, L., Street, C., Li, Y., Poidevin, M., Wu, H. et al. (2013). Genome-wide profiling of 5-formylcytosine reveals its roles in epigenetic priming. *Cell* **153**, 678-691.

Spruijt, C. G., Gnerlich, F., Smits, A. H., Pfaffeneder, T., Jansen, P. W., Bauer, C., Münzel, M., Wagner, M., Müller, M., Khan, F. et al. (2013). Dynamic readers for 5-(hydroxy)methylcytosine and its oxidized derivatives. *Cell* **152**, 1146-1159.

Stadtfeld, M., Apostolou, E., Akutsu, H., Fukuda, A., Follett, P., Natesan, S., Kono, T., Shioda, T. and Hochedlinger, K. (2010). Aberrant silencing of imprinted genes on chromosome 12qF1 in mouse induced pluripotent stem cells. *Nature* **465**, 175-181.

Suzuki, M. M. and Bird, A. (2008). DNA methylation landscapes: provocative insights from epigenomics. *Nat. Rev. Genet.* **9**, 465-476.

Thorvaldsdóttir, H., Robinson, J. T. and Mesirov, J. P. (2013). Integrative Genomics Viewer (IGV): high-performance genomics data visualization and exploration. *Brief. Bioinform.* **14**, 178-192.

Wang, W., Lin, C., Lu, D., Ning, Z., Cox, T., Melvin, D., Wang, X., Bradley, A. and Liu, P. (2008). Chromosomal transposition of PiggyBac in mouse embryonic stem cells. *Proc. Natl. Acad. Sci. USA* **105**, 9290-9295.

Williams, K., Christensen, J., Pedersen, M. T., Johansen, J. V., Cloos, P. A., Rappsilber, J. and Helin, K. (2011). TET1 and hydroxymethylcytosine in transcription and DNA methylation fidelity. *Nature* **473**, 343-348.

Woltjen, K., Michael, I. P., Mohseni, P., Desai, R., Mileikovsky, M., Hämäläinen, R., Cowling, R., Wang, W., Liu, P., Gertsenstein, M. et al. (2009). piggyBac transposition reprograms fibroblasts to induced pluripotent stem cells. *Nature* **458**, 766-770.

Wu, S. C. and Zhang, Y. (2010). Active DNA demethylation: many roads lead to Rome. *Nat. Rev. Mol. Cell Biol.* **11**, 607-620.

Wu, H., D'Alessio, A. C., Ito, S., Xia, K., Wang, Z., Cui, K., Zhao, K., Sun, Y. E. and Zhang, Y. (2011). Dual functions of Tet1 in transcriptional regulation in mouse embryonic stem cells. *Nature* **473**, 389-393.

Yamaguchi, S., Hong, K., Liu, R., Shen, L., Inoue, A., Diep, D., Zhang, K. and Zhang, Y. (2012). Tet1 controls meiosis by regulating meiotic gene expression. *Nature* **492**, 443-447.

Yamaji, M., Seki, Y., Kurimoto, K., Yabuta, Y., Yuasa, M., Shigeta, M., Yamanaka, K., Ohinata, Y. and Saitou, M. (2008). Critical function of Prdm14 for the establishment of the germ cell lineage in mice. *Nat. Genet.* **40**, 1016-1022.

Yamaji, M., Ueda, J., Hayashi, K., Ohta, H., Yabuta, Y., Kurimoto, K., Nakato, R., Yamada, Y., Shirahige, K. and Saitou, M. (2013). PRDM14 ensures naive pluripotency through dual regulation of signaling and epigenetic pathways in mouse embryonic stem cells. *Cell Stem Cell* **12**, 368-382.